
# Run time acceleration for adaptive algorithm for OFDM bit-loading for OWC channels

**T. E. Bitencourt Cunha[1] and J. P. M. G. Linnartz[1,3]**
[1]Eindhoven University of Technology, 5600 MB Eindhoven, The Netherlands
[2]Universitat Politècnica de València, Valencia, Spain
[3]Signify (Philips Lighting) Research, 5656 AE Eindhoven, The Netherlands
{t.e.bitencourt.cunha, J.P.linnartz}@tue.nl, j.p.linnartz@signify.com

DRAFT VERSION FOR REVIEWING PURPOSES

Motivated by their low cost, LED light sources are popular in the design of OWC systems. To support new applications and to handle the ever-increased number of devices connected to the network, the goal migrates from the development of systems to deliver the highest possible bit rate ($bit/s$) to networks that deliver the highest possible bit rate density, i.e., $bit/s/m^2$. Looking into an individual emitter, the covered area by it becomes particularly important. Hence, the trade-off between optical output power (high range and coverage area) and transmission bandwidth is of particular importance [1, 2].

By increasing the current density ($A/cm^2$), the carrier recombination in the LED quantum well can be accelerated and, consequently, the transmission bandwidth is extended. However, at high levels it may also induce undesired effects such as reduced efficiency and increased temperature of the junction, which may reduce system performance [1]. Many studies have shown impressive throughput values with the large bandwidths achieved using micro-LEDs [3, 4]. However, most of the experiments only report short range links within a small coverage area, where low optical output power may not be a limitation. To support mobility within a larger coverage area, larger and more efficient LEDs may be preferred, operated at lower output power, even though these may have a narrower cut-off frequency. Meanwhile, the capacitance of photo diodes may lead to poorer performance at high modulation frequencies. Similarly, small delays due to multipath reception of light may be experienced as a roll-off of the channel response, particularly in a non-line of sight link. To optimize OWC systems for 6G requirements, techniques to overcome the low-pass frequency response of the light sources have been studied [5].

The narrow 3-dB bandwidth of larger LEDs may impose a bottleneck for the system to achieve high bit rates. However, usually, the roll-off above the 3-dB bandwidth is gentle (first order) which may be mitigated by a pre-emphasis. Pre-emphasis aims to

speed up the LED response by inverting the low-pass frequency response of the device. However, it may be counterproductive as it inefficiently emphasizes modulation power at higher frequencies. In contrast to this, a Lagrangian optimization of the throughput, by adaptive bit and power loading advises to modulate the LED far beyond its 3 dB bandwidth, but at reduced (rather than emphasized) modulation power at higher frequencies [6]. Doing this, the power budget is efficiently spent to improve the data rate [5].

Orthogonal frequency division multiplexing (OFDM) is a known modulation scheme which supports the allocation of power and data payload per frequency bin taking the channel response at all frequencies into account. With OFDM, multiple independent subcarriers are simultaneously transmitted. Considering the need for a real-valued transmit signal vector, for a total of $N_S = N_{FFT}/2$ transmitted independent complex-valued symbols using an FFT of size $N_{FFT}$, the system sum-rate can be estimated by

$$R = \max_{\tilde{\sigma}_l^2(k)} \Delta_B \sum_{k=1}^{N_S} \log_2\left(1 + \frac{\boldsymbol{h}(k)^2 \boldsymbol{P}(k)}{\Gamma \boldsymbol{N}_0(k) \Delta_B}\right) \quad (1)$$
$$\text{s. t.} \sum_{k=1}^{N_S} P(k) \leq P_T$$

where $\boldsymbol{h}(k)$, $\boldsymbol{P}(k)$ and $\boldsymbol{N}_0(k)$ correspond, respectively, to the (real-valued) channel gain, the modulation power, and the noise power on a $k$-th OFDM sub-carrier. The coefficient $\Delta_B$ represents the sub-carrier bandwidth and $\Gamma$ models the SNR gap due to a required BER performance. The power allocation is restricted to a power budget, then we have the power constraint $\sum_{k=1}^{N_S} P(k) \leq P_T$, where $P_T$ is the power limitation of the LED.

To reduce the overhead due to the inherent complexity of solving the optimization problem for $N_S$ variables $\boldsymbol{P}(k)$, we studied methods to accelerate the solving of (1) in real scenarios. Also, concerns such as hardware costs and energy consumption motivate the design of algorithms able to achieve the best balance between computing $\boldsymbol{P}(k)s$ for a satisfactory throughput performance and the computational complexity for doing so.

Several studies have proposed different strategies to solve (1) considering that the channel response is a continuous function of frequency, i.e. $\Delta_B \to 0$ and $N_S \to \infty$, that rate is a continuous function of the SNR and that $\boldsymbol{N}_0(k)$ is flat over the frequency response. Note that in the continuous case, (1) becomes an integral instead of a limited sum, which could be solved specific channel models. In fact, experimental models have been proposed for the LED frequency response, and these allow analytical expressions for the power loading, in particular for a first-order low-pass filter [7] or for an exponential decay of the frequency response [5]. Although quite useful to quantify and compare system choices, in real systems these expressions might be overly simplified and may not work to fixed bit loading and power loading profiles. Moreover, these may not capture all effects in the communication channel. Firstly, analysis of OWC receivers, e.g., including PD arrays and a transimpedance amplifier (TIA) response, show colored noise power spectral densities [8]. In addition, in a real system the number of bits that can be allocated into each subcarrier is limited to integer numbers, using integer powers of two for the constellation size of QAM symbols. In practice, subcarriers that carry less

than one bit are useless or very hard to exploit. In the continuous case, if an average is taken over the number of bits allocated per frequency bin, a value lower than or equal to one may appear, which is unrealistic. These concerns highlight the importance of power and bit allocation algorithms for generic discrete channels $\boldsymbol{h}(k)$ with non-white noise $\boldsymbol{N}_0(k)$ and considering the discrete nature of bit allocation.

Since problem (1) is convex, one may think to use optimization solvers such as CVX to compute the best power allocation pattern. Although very powerful, the complexity of CVX shows to be impractical to handle with compute restricted chipsets. On the development of methods that are able to solve the problem with lower computational cost but with near optimal performance, our recent research, e.g. also in [9], explores how the Huges-Hartogs algorithm [10] can be adapted and accelerated. The algorithm is based on the computation of the costs in power to allocate bits over the sub-carriers. The throughput of the system can be seen as a sum of the rates achieved by each orthogonal subcarrier. As illustrated in Figure 2, at an $k$-th subcarrier, a small increment in power $\triangle_{\boldsymbol{P}(k)}$ can lead to a proportional increment in throughput of $\triangle_{\boldsymbol{R}(k)}$ bits.

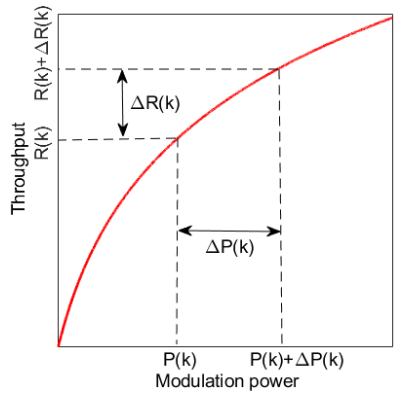


Figure 1: Illustration of throughput vs power at an $k$-th OFDM subcarrier.

In the discrete case, to achieve the high throughput for a given power budget, the algorithm loads at each iteration power into the sub-carrier with the lowest cost to increase the sum-rate in one bit. According to our interpretation, it may have been inspired by the KKT condition which says that, for a continuous channel, at an optimum, derivatives $dR/dP(k)$ are either equal for all k or $P(k) = 0$. Indeed, a Lagrangian optimization ensures that, at an optimal solution, any possible incremental extra bit in throughput obtained per unit of extra power that would be allocated to any specific subcarrier becomes equal for all used subcarriers [11]. At a $k$-th sub-carrier the extra power $\triangle_{\boldsymbol{P}(k)}$ required per an extra number of bits $\triangle_{\boldsymbol{R}(k)}$ can be estimated by

$$\frac{\triangle_{\boldsymbol{R}(k)}}{\triangle_{\boldsymbol{P}(k)}} \approx \frac{\Delta_B \log_2\left(1+\frac{\boldsymbol{h}(k)^2\left(\boldsymbol{P}(k)+\triangle_{\boldsymbol{P}(k)}\right)}{\Gamma \boldsymbol{N}_0(k)\Delta_B}\right) - \Delta_B \log_2\left(1+\frac{\boldsymbol{h}(k)^2\boldsymbol{P}(k)}{\Gamma \boldsymbol{N}_0(k)\Delta_B}\right)}{\triangle_{\boldsymbol{P}(k)}} \qquad (2)$$

The computation of (2) can be simplified by defining the gain to noise ratio (GNR) as $\boldsymbol{a}(k) = \boldsymbol{h}(k)^2/\Gamma \boldsymbol{N}_0(k)\Delta_B$. This gives,

$$\frac{\triangle R(k)}{\Delta_B} \approx \log_2\left(1 + a(k)\left(\boldsymbol{P}(k) + \triangle_{P(k)}\right)\right) - \log_2\left(1 + a(k)\boldsymbol{P}(k)\right)$$
$$\approx \log_2\left(\frac{1 + a(k)\left(\boldsymbol{P}(k) + \triangle_{P(k)}\right)}{1 + a(k)\boldsymbol{P}(k)}\right) \quad (3)$$

Removing the $\log_2(\cdot)$ dependence of the equation results in

$$2^{\frac{\triangle \boldsymbol{R}(k)}{\Delta_B}} \approx \frac{1 + a(k)\left(\boldsymbol{P}(k) + \triangle_{\boldsymbol{P}(k)}\right)}{1 + a(k)\boldsymbol{P}(k)} \quad (4)$$

Our goal is to achieve an expression for $\triangle_{\boldsymbol{P}(k)}$, thus isolating it into one side of the equation, which requires some operations such as

$$1 + a(k)\left(\boldsymbol{P}(k) + \triangle_{\boldsymbol{P}(k)}\right) \approx 2^{\frac{\triangle \boldsymbol{R}(k)}{\Delta_B}}\left(1 + a(k)\boldsymbol{P}(k)\right) \quad (5)$$

In (5) it is possible to observe a common term $\left(1 + a(k)\boldsymbol{P}(k)\right)$ at both sides. This can then be simplified to

$$a(k)\ \triangle_{\boldsymbol{P}(k)} = \left(1 + a(k)\boldsymbol{P}(k)\right)\left(2^{\frac{\triangle \boldsymbol{R}(k)}{\Delta_B}} - 1\right) \quad (6)$$

Isolating the power cost $\triangle_{\boldsymbol{P}(k)}$ at one side leads to

$$\triangle_{\boldsymbol{P}(k)} = \left(\frac{1}{a(k)} + \boldsymbol{P}(k)\right)\left(2^{\frac{\triangle \boldsymbol{R}(k)}{\Delta_B}} - 1\right) \quad (7)$$

In the last step we insert back the GNR $a(k)$ into (7), which ends equal to

$$\triangle_{\boldsymbol{P}(k)} = \left(\frac{\Gamma \boldsymbol{N}_0(k)\Delta_B}{\boldsymbol{h}(k)^2} + \boldsymbol{P}(k)\right)\left(2^{\frac{\triangle \boldsymbol{R}(k)}{\Delta_B}} - 1\right) \quad (8)$$

Equation (8) gives to us a metric to estimate the cost in power $\triangle P(k)$ to increment the number of bits loaded at sub-carrier k in $\triangle R(k)/\Delta_B$ bits. As the throughput is composed by the sum of the rates achieved at each independent subcarrier it also corresponds to increment the overall data rate into $\triangle R/\Delta_B$ bits. Considering $\triangle R(k)/\Delta_B$ small as one bit, (8) becomes

$$\triangle_{\boldsymbol{P}(k)} = P(k) + \frac{\Gamma \boldsymbol{N}_0(k)\Delta_B}{\boldsymbol{h}(k)^2} \quad (9)$$

Evidently, evaluation of the above equation is much faster than calculation of (2).

We further interpret this a follows: at an *i*-th iteration, the amount of power required to increase throughput in 1 bit is a function of the amount of power $P(k)$ required to allocate a certain number of bits in previous iterations (or in fact just equal to $P(k)$ ), plus a channel-dependent constant $\Gamma \boldsymbol{N}_0(k)\Delta_B/\boldsymbol{h}(k)^2$. Note that the term on the right in (9) is a channel property, independent of the iterations so it can be pre-computed and saved in an array of size $N_S$.

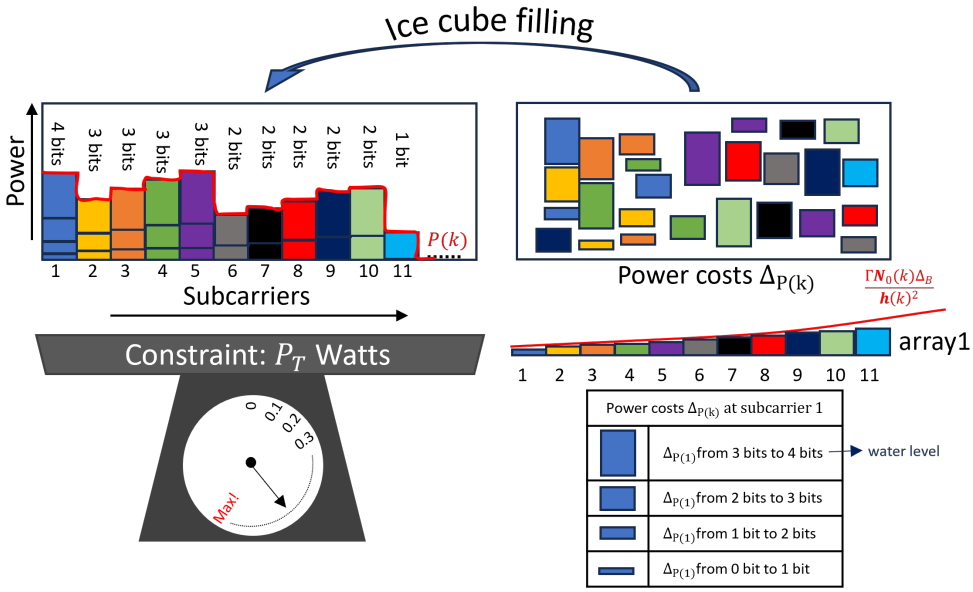


Figure 2: Illustrative representation of the Ice cube filling algorithm.

**Ice cube filling**

As the bit allocation processes discrete quantities, we can interpret this as filling recipients (subcarriers) with cubes (power costs) while measuring the weight of all recipients (power constraint) every time at which a cube is placed inside to one recipient (power allocation). An illustrative representation is shown in Figure 2.

We can relate this to the waterfiling principle:

- In (9), the inverted channel profile is $\Gamma \boldsymbol{N}_0(k)\Delta_B \,/\, \boldsymbol{h^2}(k)$.
- There is a double role for $\triangle_{\boldsymbol{P}(k)}$. As said above, it can be interpreted as the extra power, but thinking in terms of waterfilling it can be seen as the "water level". In fact, the power $P(k)$ in (9) added to the inverted channel profile which is a constant value. If every iteration searches for the value of $\triangle_{\boldsymbol{P}(k)}$ where the smallest step can be made, the series of $\triangle_{\boldsymbol{P}(k)}$ as a function of $k$ tends towards a constant. In other words, HH is exactly the same as trying to fulfill KKT and also equivalent to iteratively filling a water level (though it may rather be seen as filling with "ice cubes" of finite discrete (non-infinitesimal) size.

**Memory utilization and reducing the number of computations**

If the received signal strength changes, e.g. because of motion or rotation of a client device, the system needs to recalculate bit loading. Thus, finding ways to accelerate the algorithms can improve performance and power consumption.

Firstly, we observe that the effect of the channel needs to be pre-processed once, by calculating the array of $N_S$ entries from $\mathrm{k} = 1, \ldots, N_S$, denoted here as **Array1**(k)= $\Gamma \boldsymbol{N}_0(k)\Delta_B \,/\, \boldsymbol{h^2}(k)$. Secondly, more tree arrays are required. The system also needs to memorize an array for the power costs $\triangle_{\boldsymbol{P}}$ and another one $\boldsymbol{p}$ with the power loaded. As

it is important to determine the constellation size (or equivalently , the number of bits) for each OFDM subcarrier, a last array $\boldsymbol{b}$ is also required.

**Further acceleration**

The algorithm stops when the power budget is completely spent. To speed up the algorithm we show that, indeed, there is a need to compute the additional cost to increase the data rate by one bit for all sub-carriers but only once per OFDM frame. Iteratively, the sub-carrier with lowest cost is searched, and the cost to increase one bit into is updated. Thus, in fact only for one subcarrier a new cost function needs to be calculated, rather than that all subcarriers need to be revisited. The power allocation pattern is then computed bit by bit with a drastically reduced computational cost per iteration. In general, the average running time of the algorithm can be many orders of magnitude lower than commonly used approaches. The algorithm is illustrated in Algorithm 1.

**Algorithm 1**: Accelerated HH algorithm

**Input**: $\Gamma, \boldsymbol{N}_0, \Delta_B, N_S, \boldsymbol{h}^2, P_T$

Initialization: $\mathbf{array1}(k), \triangle_{\boldsymbol{P}} \leftarrow \frac{\Gamma \boldsymbol{N_0}(k)\Delta_B}{\boldsymbol{h}(k)^2},\ \nabla k = 1, \dots, N_S$

$\mathbf{p}, \mathbf{b} \leftarrow \mathbf{0}\ , \nabla k = 1, \dots, N_S$

$\text{constraint} = 0$

$(k) = \min(\triangle_{\boldsymbol{P}})$

$\text{constraint} = \text{constraint} + \triangle_{\boldsymbol{P}}\ (k)$

**while** $\text{constraint} \leq P_T$ %check power constraint

$\mathbf{p}(k) = \mathbf{p}(k) + \triangle_{\boldsymbol{P}}\ (k)$ %update power allocation array

$\mathbf{b}(k) = \mathbf{b}(k) + 1$ %update bit allocation array

$\triangle_{\boldsymbol{P}}\ (k) = \mathbf{p}(k) + \mathbf{Array1}(k)$ %update power costs array (9)

$(k) = \min(\triangle_{\boldsymbol{P}})$ %selects the subcarrier with minimum cost

$\text{constraint} = \text{constraint} + \triangle_{\boldsymbol{P}}\ (k)$ %update power constraint

**End**

**Output: p, b**

Where $\min(\triangle_{\boldsymbol{P}})$ subcarrier index , k, with lowest cost to increase the data rate in one bit.

Indeed, although Algorithm 1 simplifies the computation per-iteration, the total number of iterations for the computation of the best $\mathrm{P}(k)s$ can be still large. Considering that the channel is low-pass the amount of iterations can be drastically reduced if the performance achieved by a suboptimal solution is acceptable.

**Performance evaluation**

Besides the computation speeds, discussed above we also checked whether the algorithms reach the throughout that a full CVX would achieve. To evaluate the performance of algorithm 1, we use optimized expressions from [7] for the case where

$h(k)s$ model a well-behaved first-order low-pass frequency decay and $N_0(k)$ is flat. Considering that the channel is continuous in frequency, the maximum throughput achieved by the optimum waterfilling power allocation corresponds to

$$R_w = \frac{2f_c}{\ln 2}\left[\left(\frac{3}{2}\frac{\boldsymbol{h}_0{}^2 P_T}{\Gamma N_0 f_c}\right)^{\frac{1}{3}} - \tan^{-1}\left(\left(\frac{3}{2}\frac{\boldsymbol{h}_0{}^2 P_T}{\Gamma N_0 f_c}\right)^{\frac{1}{3}}\right)\right] \tag{10}$$

where the power spectrum density is given by

$$\mathrm{P(k)} = \frac{N_0}{f_c{}^2}(f_{max_w}{}^2 - f_k{}^2) \tag{11}$$

and the optimum maximum modulation frequency is computed as

$$f_{max_w} = f_c\left(\frac{3}{2}\frac{\boldsymbol{h}_0{}^2 P_T}{N_0 f_c}\right)^{\frac{1}{3}} \tag{12}$$

The coefficients $P_T$ and $f_c$ in (3) and (5) correspond to the link power budget and the LED 3-dB bandwidth. $f_k$ in (4) represents the frequency at the $k$-th OFDM subcarrier.

For further evaluation, we also estimate the throughput that could be achieved by solving (1) with the convex optimization software solution CVX [12]. Figure 3 shows the throughput achieved for different values of power link budget $\gamma_{TX}$ defined as

$$\gamma_{TX} = \frac{P_T}{N_0 f_c} \tag{13}$$

Figure 3 shows the throughput achieved by each power allocation solution analyzed. The difference with the analytical water filling expression is small and it presumably due to the discrete character of the "cubes" and of the inability to use subcarriers with very low SNR at less than one bit. Moreover, WF assumes an infinite summation over the frequency response up to a maximum optimized signal bandwidth, which contradicts the finite number of subcarriers. As can be observed the throughput achieved by both CVX and by the Ice cube filling algorithm is almost the same, for a slightly, almost not visible, higher throughput for CVX. This can be justified by the fact that, although both consider a finite number of subcarriers, for CVX the granularity of bits on the rate expression is lower than one. So, CVX is able to fully use the power budget while for Ice cube filling algorithm at the end of the iterative process a small portion of it can not be used. The Uniform curve represents the uniform allocation of power where no optimization is done, P(k) is simply equal to $P_T/N_S$ for all subcarriers. The lowest performance achieved by Uniform highlights the importance of a power allocation algorithm to overcome the loss in performance dua to the low-pass channel response.

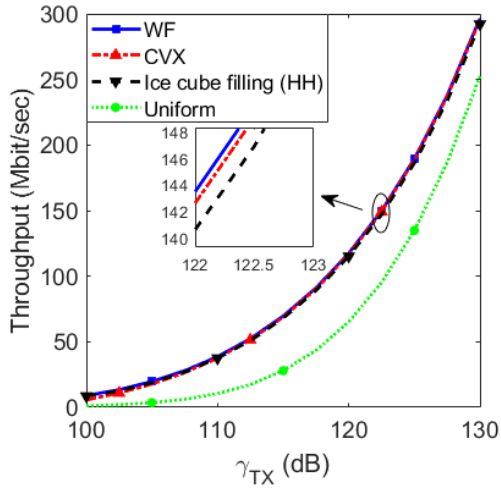


Figure 3: LED-based OFDM OWC system considering white noise for different link budgets $\gamma_{TX}$. Simulation parameters: $f_c = 10$ MHz, $\Gamma = 6.06$, $h_0 = 2.0\text{x}10^{-5}$ and $N_0 = 10^{-22}$.

Figure 4 shows the average running time of CVX and of the Ice cube filling algorithm for the considered scenario. For computing solutions, it is possible to observe that the iterative algorithm is much faster than CVX. Although precise on computing solutions, CVX requires a huge number of operations to o reach an small approximation accuracy $\epsilon$. At the other side, the Ice cube filling algorithm requires a total of $R/\Delta_B$ iterations while each requires a search in a vector with finite length and a small number of sums.

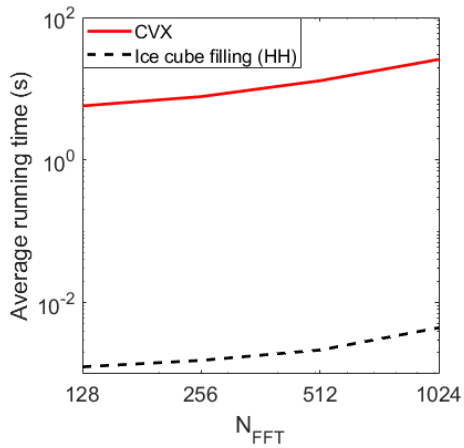


Figure 4: Average running times on a log scale for solutions computed with CVX and with the Ice cube filling algorithm. For different numbers of OFDM sub-carriers $N_{FFT}$ and for $\gamma_{TX}$ corresponding to 130 dB.

## Conclusion

Effective power and bit loading strategies are indispensable for mitigating throughput losses attributed to the low-pass frequency response of the LEDs and PDs in OWC systems. To enable the widespread adoption of a high-speed wireless technology using LEDs, the development of precise, computation-friendly algorithms is required. Although expressions for the power allocation in a continuous channel exist, these show to not be the most appropriate in real scenarios as the OWC chipsets are digital devices with finite precision. Moreover, response of the TIAs shows to distort the power spectrum density of the noise, a factor often assumed to be flat in existing expressions. In this research, we delve into the adaptation and acceleration of an iterative algorithm in the past used in RF systems to optimize performance of LED-based OWC systems. The strategy shows to be efficient, less computationally demanding then commonly used optimization solvers and it intrinsically consider the finite precision of the chipsets.

# References


[1] J. -P. M. G. Linnartz, T. E. B. Cunha, D. V. Romero and X. Deng, "Throughput optimization for IR-LEDs in an optical wireless link," in *ICC 2022 - IEEE International Conference on Communications*, 2022.

[2] D. Vargas Romero, T. E. B. Cunha and J. P. Linnartz, "Optimizing LED Performance for LiFi: Bandwidth versus Efficiency," in *26th Annual Symposium of the IEEE Photonics Benelux Chapter*, Eindhoven, Netherlands, 2022.

[3] D. Tsonev et al., "A 3-Gb/s Single-LED OFDM-Based Wireless VLC Link Using a Gallium Nitride µLED," *IEEE Photonics Technology Letters,* vol. 26, no. 7, pp. 637-640, 2014.

[4] M. S. Islim et al., "Towards 10 Gb/s orthogonal frequency division multiplexing-based visible light communication using a GaN violet micro-LED," *Photon. Res.,* vol. 5, no. 2, p. A35, 2017.

[5] S. Mardanikorani, X. Deng and J. -P. M. G. Linnartz, "Sub-Carrier Loading Strategies for DCO-OFDM LED Communication," *IEEE Transactions on Communications,* vol. 2, no. 68, pp. 1101-1117, 2020.

[6] J. -P. M. G. Linnartz, X. Deng, A. Alexeev and P. v. Voorthuisen, "An LED Communication Model Based on Carrier Recombination in the Quantum Well," in *2021 IEEE 32nd Annual International Symposium on Personal, Indoor and Mobile Radio Communications (PIMRC)*, Helsinki, 2021.

[7] S. Mardani and J.-P. Linnartz, "Capacity of the first-order low-pass channel with power constraint," in *2018 Symposium on Information Theory and Signal Processing in the Benelux*, Enschede, 2018.

[8] X. Liu, J. -P. M. G. Linnartz, A. M. Khalid and K. Arulandu, "Response of a Matrix Circuit of Photodiodes with a common Transimpedance Amplifier in Optical Wireless Communications," in *2023 IEEE Wireless Communications and Networking Conference (WCNC)*, Glasgow, United Kingdom, 2023.

[9] T. E. B. Cunha and J.-P. M. G. Linnartz, "OFDM Bitloading in Distributed MIMO OWC Using Power-Constrained LEDs," *IEEE Access,* 2023.

[10] D. Hughes-Hartogs, "Ensemble modem structure for imperfect transmission media". U.S. Patent 4.833.706, May 1989.

[11] J. -P. M. G. Linnartz, X. Deng, A. Alexeev and S. Mardanikorani, "Wireless Communication over an LED Channel," *IEEE Communications Magazine,* vol. 58, no. 12, pp. 77-82, December 2020.

[12] M. Grant and S. Boyd, "CVX: Matlab software for disciplined convex programming, version 2.1," Mar. 2021. [Online]. Available: http://cvxr.com/cvx.

[13] W. Saad, M. Bennis and M. Chen, "A Vision of 6G Wireless Systems: Applications, Trends, Technologies, and Open Research Problems," *IEEE Network,* vol. 34, no. 3, pp. 134-142, 2020.

[14] H. Haas, L. Yin, Y. Wang and C. Chen, "What is LiFi?," *Journal of Lightwave Technology,* vol. 34, no. 6, pp. 1533-1544, 2016.

[15] T. Fath and H. Haas, "Performance Comparison of MIMO Techniques for Optical Wireless Communications in Indoor Environments," *IEEE Transactions on Communications,* vol. 61, no. 2, pp. 733-742, 2013.

[16] H. Chen, A. T. L. Lee, S. -C. Tan and S. Y. Hui, "Electrical and Thermal Effects of Light-Emitting Diodes on Signal-to-Noise Ratio in Visible Light Communication," *IEEE Transactions on Industrial Electronics,* vol. 66, no. 4, pp. 2785-2794, 2019.

[17] T. E. B. Cunha, J. -P. M. G. Linnartz and X. Deng, "Achievable rate of LED-based distributed MIMO OWC systems under a per-LED power constraint," in *2021 17th International Symposium on Wireless Communication Systems (ISWCS)*, 2021.

[18] Y. Zeng, J. Wang, X. Ling, X. Liang and C. Zhao, "Joint precoder and DC bias design for MIMO VLC systems," in *2017 IEEE 17th International Conference on Communication Technology (ICCT)*, 2017.

[19] J. Lian, Y. Gao, P. Wu, G. Zhu and Y. Wang, "Indoor MIMO VLC systems using optical orthogonal frequency division multiple access," *Optics Communications,* vol. 485, 2021.

[20] J. P. Linnartz et al., "ELIoT: New Features in LiFi for Next-Generation IoT," in *2021 Joint European Conference on Networks and Communications & 6G Summit (EuCNC/6G Summit)*, 2021.